Theory of two-photon down-conversion in the presence of mirrors

P. W. Milonni and H. Fearn*
Theoretical Division (T-4), Los Alamos National Laboratory, Los Alamos, New Mexico 87545

A. Zeilinger
Institut für Experimentalphysik, Universität Innsbruck, Technikerstrasse 25, A-6020, Innsbruck, Austria
(Received 26 October 1995)

A theory of two-photon down-conversion in the presence of mirrors is developed and applied to recent observations of Herzog *et al.* [Phys. Rev. Lett. **72**, 629 (1994)]. The experimentally observed results for counting and coincidence rates as functions of mirror-crystal separations are obtained, and it is shown how the same results may be derived in a simplified formulation that presumes phase-matched signal and idler modes. We account for the observed effects of the finite coherence length of the pump field as well as the signal and idler coherence lengths, which are much shorter than the pump coherence length and have a different physical origin. Our analysis also supports the interpretation of the phenomena observed as being analogous to the modification of single photon spontaneous emission of atoms in cavity QED. [S1050-2947(96)09706-5]

PACS number(s): 42.50.Ar

I. INTRODUCTION

Recent experiments have demonstrated suppression and enhancement of the rate at which entangled two-photon pairs are created by parametric down-conversion, depending on the positions of external mirrors [1]. The mirrors allow for two indistinguishable ways by which each photon pair can be created, and the interference between these alternatives produces suppression or enhancement of the pair creation. This interpretation, while allowing for a semiquantitative explanation of the experimental results for counting and coincidence rates, does not account for the finite extent of the interaction region or for the partial coherence of the down-converted light. The purpose of this paper is to present a more detailed theory of down-conversion in the presence of external mirrors.

The suppression or enhancement by mirrors of the rate of production of down-converted photons in the presence of a steady pump beam is analogous, as previously noted [1], to the modification of single-photon spontaneous emission rates [2]. In the latter, ''cavity-QED-type'' of experiment, the emitting atoms have a spatial extent that is negligible compared with the wavelength of the emitted light, so that an atom can be positioned precisely at a point corresponding to a node or crest of the (vacuum) field at the emission wavelength. Depending on whether the atom is at such a node or crest, the spontaneous-emission rate is either suppressed or enhanced compared with its free-space value. This is interpretable as either a modification of the vacuum field interacting with the atom, compared with the free-space vacuum field, or as a modification of the atom's radiation reaction field compared with its free-space form [3]. The distances d between the atom and the reflecting surfaces must be small compared with the coherence length of the spontaneous radiation in order for these surfaces to have a significant effect on the emission. (The coherence length in this case is simply $c\tau$, where τ is the radiative lifetime.) In other words, the free-space radiation rate $A=1/\tau$ must be small compared with the photon bounce rates c/d in order for the atom to ''see'' the reflecting surfaces before emitting a photon as if in free space.

In the experiments on two-photon down-conversion, however, the interaction volume within the crystal has an extent much greater than the wavelengths of the pump or down-converted fields, and so the analogy to cavity QED is not immediately obvious. Moreover, the coherence length of the down-converted light is very small (a few hundred micrometers) compared with the distances between the crystal and the external mirrors, and so again an essential feature of ordinary cavity QED is absent. Our analysis nevertheless validates the interpretation of the down-conversion experiments in the fashion of cavity QED.

The experimental setup of interest here is indicated in Fig. 1. In the following section we formulate the Hamiltonian and Heisenberg equations of motion that form the basis for the rest of the paper. In Secs. III and IV we calculate the dependence of the signal, idler, and coincidence counting rates on the crystal-mirror separations, obtaining results in agreement

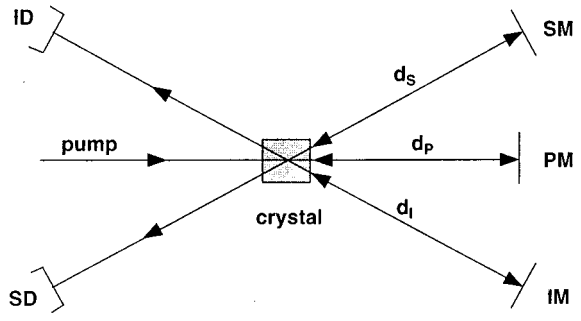

FIG. 1. Experimental configuration employed by Herzog *et al.* [1]. PM, SM, and IM are mirrors reflecting pump, signal, and idler fields, respectively, and SD and ID are signal and idler photodetectors, respectively.

*Permanent address: Department of Physics, California State University, Fullerton, CA 92634-9480.

with the observations of Herzog *et al.* [1]. The analysis is extended in Sec. V to account for the finite coherence lengths of the pump, signal, and idler fields. Section VI briefly summarizes our results and conclusions.

II. HAMILTONIAN AND HEISENBERG OPERATORS

In order to describe how the pump field interacts with the nonlinear crystal we take as our starting point the basic $-\mathbf{P}\cdot\mathbf{E}$ interaction energy density and consider the change in the induced dipole energy as the inducing field is brought from 0 to $\mathbf{E}$:

$$W=-\int d^3x\int_0^{\mathbf{E}}\mathbf{P}(\mathbf{E})\cdot d\mathbf{E}, \tag{1}$$

where $\mathbf{P}$ is the dipole moment density. In the linear case $P_i=\chi_{ij}E_j$, where the summation convention for repeated indices is used. Then

$$W=-\int d^3x\chi_{ij}\int_0^{\mathbf{E}}E_j dE_i=-\frac{1}{2}\int d^3xP_iE_i. \tag{2}$$

The factor $\frac{1}{2}$ arises because the dipole density is *induced* [4]. In the case of a second-order nonlinear polarization $P_i=\chi_{ijk}E_jE_k$ we have, similarly,

$$W=-\int d^3x\int_0^{\mathbf{E}}P_i dE_i=-\frac{1}{3}\int d^3x\chi_{ijk}\int_0^{\mathbf{E}}d(E_iE_jE_k)$$

$$=-\frac{1}{3}\int d^3x\chi_{ijk}E_iE_jE_k, \tag{3}$$

which differs from the form assumed by Hong and Mandel [5]; in their formulation a factor $\frac{1}{2}$ appears instead of the $-\frac{1}{3}$ of Eq. (3). Although the form (3) might in principle be taken as the appropriate one, the difference is immaterial, as different multiplicative factors can be reabsorbed into the definition of the nonlinear susceptibility. We will take χ_{ijk} to be independent of frequency, which is an excellent and frequently employed approximation for pump, signal, and idler frequencies far from any absorption resonances of the crystal.

The linear coupling between the matter and the field leads among other things to different refractive indices inside and outside the crystal. For simplicity, and following Hong and Mandel [5], we ignore such differences in writing the Hamiltonian and assume we have vacuum outside the crystal. Then, assuming only a *nonlinear* coupling between the crystal and the field, we use the Hamiltonian

$$H=H_{\text{matter}}+H_{\text{field}}-\frac{1}{3}\int d^3x\chi_{ijk}E_iE_jE_k$$

$$=H_{\text{matter}}+\sum_\gamma\hbar\omega_\gamma a_\gamma^\dagger a_\gamma-\frac{1}{3}\int d^3x\chi_{ijk}E_iE_jE_k, \tag{4}$$

where a_γ and $a_\gamma^\dagger$ are the usual photon annihilation and creation operators, respectively, for mode γ. The ith component of the electric field operator can be written as

$$E_i(\mathbf{x},t)=i\sum_\gamma(2\pi\hbar\omega_\gamma)^{1/2}[a_\gamma(t)U_{\gamma i}(\mathbf{x})-a_\gamma^\dagger(t)U_{\gamma i}^*(\mathbf{x})], \tag{5}$$

so that

$$H=H_{\text{matter}}+\sum_\gamma\hbar\omega_\gamma a_\gamma^\dagger a_\gamma-\frac{i^3}{3}(2\pi\hbar)^{3/2}\sum_{\gamma\beta\alpha}(\omega_\gamma\omega_\beta\omega_\alpha)^{1/2}$$

$$\times\int d^3x\chi_{ijk}[a_\gamma U_{\gamma i}(\mathbf{x})-a_\gamma^\dagger U_{\gamma i}^*(\mathbf{x})]$$

$$\times[a_\beta U_{\beta j}(\mathbf{x})-a_\beta^\dagger U_{\beta j}^*(\mathbf{x})][a_\alpha U_{\alpha k}(\mathbf{x})-a_\alpha^\dagger U_{\alpha k}^*(\mathbf{x})]. \tag{6}$$

Here the $\mathbf{U}_\gamma$ are field mode functions whose form for the problem of interest is discussed later, and i, j, k denote their Cartesian components.

In the Heisenberg picture the operators are time dependent. The photon annihilation operator for mode γ, for instance, satisfies the Heisenberg equation of motion

$$i\hbar\dot{a}_\gamma(t)=[a_\gamma,H]=\hbar\omega_\gamma a_\gamma(t)-\frac{1}{3}\int d^3x\chi_{ijk}[a_\gamma,E_iE_jE_k]. \tag{7}$$

Now

$$[a_\gamma,E_iE_jE_k]=[a_\gamma,E_i]E_jE_k+E_i[a_\gamma,E_j]E_k+E_iE_j[a_\gamma,E_k]$$

$$=-i(2\pi\hbar\omega_\gamma)^{1/2}[U_{\gamma i}^*(\mathbf{x})E_j(\mathbf{x},t)E_k(\mathbf{x},t)$$

$$+U_{\gamma j}^*(\mathbf{x})E_i(\mathbf{x},t)E_k(\mathbf{x},t)$$

$$+U_{\gamma k}^*(\mathbf{x})E_i(\mathbf{x},t)E_j(\mathbf{x},t)], \tag{8}$$

and so

$$\dot{a}_\gamma=-i\omega_\gamma a_\gamma(t)$$

$$+\frac{1}{3}\left(\frac{2\pi\omega_\gamma}{\hbar}\right)^{1/2}\int d^3x\chi_{ijk}[U_{\gamma i}^*(\mathbf{x})E_j(\mathbf{x},t)E_k(\mathbf{x},t)$$

$$+U_{\gamma j}^*(\mathbf{x})E_i(\mathbf{x},t)E_k(\mathbf{x},t)+U_{\gamma k}^*(\mathbf{x})E_i(\mathbf{x},t)E_j(\mathbf{x},t)]$$

$$=-i\omega_\gamma a_\gamma(t)$$

$$+\left(\frac{2\pi\omega_\gamma}{\hbar}\right)^{1/2}\int d^3x'\chi_{ijk}U_{\gamma i}^*(\mathbf{x}')E_j(\mathbf{x}',t)E_k(\mathbf{x}',t), \tag{9}$$

where we invoke permutation symmetry of χ_{ijk} [6]. This equation can be formally integrated to give

$$a_\gamma(t)=a_\gamma(0)e^{-i\omega_\gamma t}+\left(\frac{2\pi\omega_\gamma}{\hbar}\right)^{1/2}\int d^3x'\chi_{ijk}U_{\gamma i}^*(\mathbf{x}')$$

$$\times\int_0^t dt'E_j(\mathbf{x}',t')E_k(\mathbf{x}',t')e^{i\omega_\gamma(t'-t)}. \tag{10}$$

The total electric field has two parts—the free field corresponding to the homogeneous solution of the operator Maxwell equations, and the source field associated with the nonlinear susceptibility χ_{ijk}. We are primarily concerned here with the source term, denoted by the superscript s. This term may be written, using the second term of Eq. (10) in Eq. (5), as

$$E_n^{(s)}(\mathbf{x},t)=\int d^3x'\chi_{ijk}\int_0^t dt' E_j(\mathbf{x}',t')E_k(\mathbf{x}',t')i\sum_\gamma (2\pi\omega_\gamma)[U_{\gamma n}(\mathbf{x})U_{\gamma i}^*(\mathbf{x}')e^{i\omega_\gamma(t'-t)}-U_{\gamma n}^*(\mathbf{x})U_{\gamma i}(\mathbf{x}')e^{-i\omega_\gamma(t'-t)}]$$

$$\equiv\int d^3x'\int_0^t dt' G_{ni}(\mathbf{x},t;\mathbf{x}',t')\chi_{ijk}E_j(\mathbf{x}',t')E_k(\mathbf{x}',t'), \tag{11}$$

where we define the Green function

$$G_{ni}(\mathbf{x},t;\mathbf{x}',t')=i\sum_\gamma (2\pi\omega_\gamma)[U_{\gamma n}(\mathbf{x})U_{\gamma i}^*(\mathbf{x}')e^{i\omega_\gamma(t'-t)} - U_{\gamma n}^*(\mathbf{x})U_{\gamma i}(\mathbf{x}')e^{-i\omega_\gamma(t'-t)}]. \tag{12}$$

Our expression for $E_n^{(s)}(\mathbf{x},t)$ is generally valid for any three-wave mixing process involving the nonlinear susceptibility χ_{ijk}. Moreover, all fields thus far are fully quantized and no assumptions have been made about the mode functions. From Eq. (10) and the general expression (5) for the electric-field operator we find for the free field, in the absence of the crystal or other sources,

$$E_n^{(0)}(\mathbf{x},t)=i\sum_\gamma (2\pi\hbar\omega_\gamma)^{1/2}[a_\gamma(0)e^{-i\omega_\gamma t}U_{\gamma n}(\mathbf{x}) - a_\gamma^\dagger(0)e^{i\omega_\gamma t}U_{\gamma n}^*(\mathbf{x})]. \tag{13}$$

From the canonical commutation relation $[a_\gamma,a_{\gamma'}^\dagger]=\delta_{\gamma\gamma'}$ for the mode annihilation and creation operators it follows straightforwardly that the Green function (12) can also be written as

$$G_{ni}(\mathbf{x},t;\mathbf{x}',t')=\frac{i}{\hbar}[E_n^{(0)}(\mathbf{x},t),E_i^{(0)}(\mathbf{x}',t')]. \tag{14}$$

In the case of free space, for which the mode functions $U_{\gamma i}(\mathbf{x})\propto\epsilon_{\gamma i}\exp(i\mathbf{k}_\gamma\cdot\mathbf{x})$, with $\hat{\boldsymbol{\epsilon}}_\gamma$ a unit polarization vector, the commutator is the well known ''Pauli-Jordan commutator'' [3]. In the case of interest here the free-space mode functions are modified by reflections off the signal, pump, and idler mirrors (Fig. 1), and the Green function will be more complicated.

III. SIGNAL AND IDLER COUNTS

Let us now apply these expressions specifically to the signal field in the three-wave mixing process in which pump radiation is down-converted in frequency to signal and idler radiation. The mode functions, and therefore the Green function in Eq. (11), will remain unspecified until we apply our results to the situation illustrated in Fig. 1. From Eqs. (11) and (13) we have

$$E_n(\mathbf{x},t)=E_n^{(0)}(\mathbf{x},t)+E_n^{(s)}(\mathbf{x},t) =E_n^{(0)}(\mathbf{x},t)+\int d^3x'\int_0^t dt' G_{ni}(\mathbf{x},t;\mathbf{x}',t')\chi_{ijk} \times E_j(\mathbf{x}',t')E_k(\mathbf{x}',t') \tag{15}$$

for the nth Cartesian component of the electric-field operator. We will be interested specifically in the case of type-I phase matching [6] in a negative uniaxial crystal. The signal and idler fields, which of course are defined arbitrarily in this context, are polarized as ordinary waves and the pump is polarized as an extraordinary wave. Then for notational convenience we can drop the subscripts on the fields in (15): $E_j(\mathbf{x}',t')$ is replaced by the pump field $E_P(\mathbf{x}',t)$, $E_k(\mathbf{x}',t')$ by the idler field $E_I(\mathbf{x}',t')$, and $E_n(\mathbf{x},t)$ by the signal field $E_S(\mathbf{x},t)$, each of these fields corresponding to specific Cartesian components taking part in the phase-matched down-conversion. Thus

$$E_S(\mathbf{x},t)=E_S^{(0)}(\mathbf{x},t) + \int d^3x'\chi\int_0^t dt' G(\mathbf{x},t;\mathbf{x}',t')E_P(\mathbf{x}',t')E_I(\mathbf{x}',t'), \tag{16}$$

where

$$G(\mathbf{x},t;\mathbf{x}',t')=i\sum_s (2\pi\omega_s)[U_s(\mathbf{x})U_s^*(\mathbf{x}')e^{i\omega_s(t'-t)} - U_s^*(\mathbf{x})U_s(\mathbf{x}')e^{-i\omega_s(t'-t)}] \tag{17}$$

and the subscript s now distinguishes among all possible *signal* modes.

The quantity of interest for the signal counting is $\langle E_S^{(-)}\times(\mathbf{x},t)E_S^{(+)}(\mathbf{x},t)\rangle$, where $(+)$ and $(-)$ designate positive- and negative-frequency parts, respectively, of the signal field operator. The positive-frequency part of the first term on the righthand side of Eq. (16) is simply

$$E_S^{(0,+)}(\mathbf{x},t)=i\sum_s (2\pi\hbar\omega_s)^{1/2}a_s(0)U_s(\mathbf{x})e^{-i\omega_s t}. \tag{18}$$

The positive-frequency part of the second (source) term in Eq. (16) is approximately

$$\int d^3x'\chi\int_0^t dt' G^{(+)}(\mathbf{x};t;\mathbf{x}',t')E_P^{(+)}(\mathbf{x}',t')E_I^{(-)}(\mathbf{x}',t'), \tag{19}$$

where

$$G^{(+)}(\mathbf{x},t;\mathbf{x}',t')\equiv i\sum_s (2\pi\omega_s)U_s(\mathbf{x})U_s^*(\mathbf{x}')e^{i\omega_s(t'-t)}. \tag{20}$$

This identification of the positive-frequency part of the signal field operator assumes that the initial state of the pump field has a narrow distribution of initially occupied states,

and furthermore for given emission directions that phase matching and energy conservation limit the range of signal and idler frequencies to narrow widths about ω_S and ω_I, respectively, where $\omega_S+\omega_I=\omega_P$, ω_P being the central frequency of the quasimonochromatic pump. In other words, we anticipate that

$$E_P^{(+)}(\mathbf{x}',t')E_I^{(-)}(\mathbf{x}',t')e^{i\omega_s t'} \tag{21}$$

is in effect slowly varying as $\exp[-i(\omega_P-\omega_I-\omega_s)t']$ for a quasimonochromatic pump and phase-matched down-conversion, so that the operator (19) varies predominantly as $\exp(-i\omega_s t)$ with $\omega_s\approx\omega_S$. Then, since

$$E_S^{(0,+)}(\mathbf{x},t)|\psi\rangle=\langle\psi|E_S^{(0,-)}(\mathbf{x},t)=0 \tag{22}$$

for an initial field state $|\psi\rangle$ with no occupied signal modes, we have for such a state

$$\langle E_S^{(-)}(\mathbf{x},t)E_S^{(+)}(\mathbf{x},t)\rangle=\int d^3x'\chi\int d^3x''\chi\int_0^t dt'\int_0^t dt''G^{(+)}(\mathbf{x},t;\mathbf{x}',t')^*G^{(+)}(\mathbf{x},t;\mathbf{x}'',t'')\langle E_I^{(+)}(\mathbf{x}',t')E_P^{(-)}(\mathbf{x}',t')E_P^{(+)}$$
$$\times(\mathbf{x}'',t'')E_I^{(-)}(\mathbf{x}'',t'')\rangle. \tag{23}$$

The lowest-order approximation to Eq. (23) involves the replacement of the field operators in the integrand by the corresponding *free* fields. This amounts to ignoring pump depletion and retaining only terms up to second order in the nonlinear susceptibility. In this approximation

$$\langle E_I^{(+)}(\mathbf{x}',t')E_P^{(-)}(\mathbf{x}',t')E_P^{(+)}(\mathbf{x}'',t'')E_I^{(-)}(\mathbf{x}'',t'')\rangle\rightarrow\langle E_I^{(0,+)}(\mathbf{x}',t')E_P^{(0,-)}(\mathbf{x}',t')E_P^{(0,+)}(\mathbf{x}'',t'')E_I^{(0,-)}(\mathbf{x}'',t'')\rangle$$
$$=\langle E_P^{(0,-)}(\mathbf{x}',t')E_P^{(0,+)}(\mathbf{x}'',t'')E_I^{(0,+)}(\mathbf{x}',t')E_I^{(0,-)}(\mathbf{x}'',t'')\rangle, \tag{24}$$

where we have used the fact that the free-field operators for different modes commute. For the initial field state $|\psi\rangle$ with no occupied idler (or signal) modes we have

$$E_I^{(0,+)}(\mathbf{x}',t')E_I^{(0,-)}(\mathbf{x}'',t'')|\psi\rangle=\sum_i\sum_{i'}(2\pi\hbar\omega_i)^{1/2}(2\pi\hbar\omega_{i'})^{1/2}U_i(\mathbf{x}')U_{i'}^*(\mathbf{x}'')a_i(0)a_{i'}^\dagger(0)e^{i\omega_{i'}t''}e^{-i\omega_i t'}|\psi\rangle$$
$$=\sum_i(2\pi\hbar\omega_i)U_i(\mathbf{x}')U_i^*(\mathbf{x}'')e^{i\omega_i(t''-t')}|\psi\rangle, \tag{25}$$

where i labels different possible idler modes. Thus

$$\langle E_P^{(0,-)}(\mathbf{x}',t')E_P^{(0,+)}(\mathbf{x}'',t'')E_I^{(0,+)}(\mathbf{x}',t')E_I^{(0,-)}(\mathbf{x}'',t'')\rangle$$
$$=\sum_i(2\pi\hbar\omega_i)U_i(\mathbf{x}')U_i^*(\mathbf{x}'')e^{i\omega_i(t''-t')}\sum_p\sum_{p'}(2\pi\hbar\omega_p)^{1/2}(2\pi\hbar\omega_{p'})^{1/2}U_p^*(\mathbf{x}')U_{p'}(\mathbf{x}'')e^{i(\omega_p t'-\omega_{p'}t'')}\langle\psi|a_p^\dagger(0)a_{p'}(0)|\psi\rangle$$
$$=\sum_i\sum_p(2\pi\hbar\omega_i)(2\pi\hbar\omega_p)U_i(\mathbf{x}')U_i^*(\mathbf{x}'')U_p^*(\mathbf{x}')U_p(\mathbf{x}'')N_p e^{i(\omega_p-\omega_i)(t'-t'')}, \tag{26}$$

where N_p is the photon number expectation value for pump mode p over the initial field state $|\psi\rangle$. We are assuming that the pump field has no mode-mode correlations, so that $\langle\psi|a_p^\dagger(0)a_{p'}(0)|\psi\rangle=\delta_{pp'}\langle\psi|a_p^\dagger(0)a_p(0)|\psi\rangle=\delta_{pp'}N_p$. Equation (23) therefore becomes

$$\langle E_S^{(-)}(\mathbf{x},t)E_S^{(+)}(\mathbf{x},t)\rangle$$
$$=(2\pi\hbar)^2\sum_i\sum_p\omega_i\omega_p N_p\int d^3x'\chi\int d^3x''\chi U_i(\mathbf{x}')U_i^*(\mathbf{x}'')U_p^*(\mathbf{x}')U_p(\mathbf{x}'')$$
$$\times\int_0^t dt'\int_0^t dt''e^{i(\omega_p-\omega_i)(t'-t'')}G^{(+)}(\mathbf{x},t;\mathbf{x}',t')^*G^{(+)}(\mathbf{x},t;\mathbf{x}'',t'')$$
$$=(2\pi\hbar)^2\sum_i\omega_i\int d^3x'\chi\int d^3x''\chi U_i(\mathbf{x}')U_i^*(\mathbf{x}'')\int_0^t dt'\int_0^t dt''G^{(+)}(\mathbf{x},t;\mathbf{x}',t')^*G^{(+)}$$
$$\times(\mathbf{x},t;\mathbf{x}'',t'')e^{-i\omega_i(t'-t'')}\sum_p N_p\omega_p U_p^*(\mathbf{x}')U_p(\mathbf{x}'')e^{i\omega_p(t'-t'')}. \tag{27}$$

The most important experimental results of Herzog *et al.* [1] can be obtained with some substantial simplifications of these general results, as we now show.

A. Mode functions

We will make the simplifying assumption of normal incidence of the fields at all mirror surfaces (PM, SM, and IM) shown in Fig. 1. Because small-aperture collimating diaphragms are employed in the experiments [1], we will assume that each pump, signal, and idler mode is characterized by one direction of propagation (**k**) plus the reflected, opposite direction. Thus the pump mode, for instance, is assumed to have the form

$$U_p(\mathbf{x}) = C_p[e^{ik_p z} - e^{ik_p(2d_P - z)}], \tag{28}$$

where C_p is a normalization factor and d_P is the distance from the crystal to the pump mirror PM in Fig. 1. The modes (28) correspond simply to the incident pump plus its reflection, and are taken to vanish at the surface of the pump mirror, where $z = d_P$. (The origin of coordinates here may be chosen arbitrarily without affecting any of our results, which only involve differences of the distances d_P, d_I, and d_S.) We can write (28) equivalently as

$$U_p(\mathbf{x}) = C_p[e^{i\mathbf{k}_p\cdot\mathbf{x}} - e^{i\phi_p}e^{-i\mathbf{k}_p\cdot\mathbf{x}}], \tag{29}$$

where $\phi_p = 2\omega_p d_P/c$ and $\mathbf{k}_p = k_p\hat{z}$. Exactly analogous expressions apply to the signal and idler modes:

$$U_s(\mathbf{x}) = C_s[e^{i\mathbf{k}_s\cdot\mathbf{x}} - e^{i\phi_s}e^{-i\mathbf{k}_s\cdot\mathbf{x}}], \tag{30}$$

$$U_i(\mathbf{x}) = C_i[e^{i\mathbf{k}_i\cdot\mathbf{x}} - e^{i\phi_i}e^{-i\mathbf{k}_i\cdot\mathbf{x}}], \tag{31}$$

where $\phi_s = 2\omega_s d_S/c$, $\phi_i = 2\omega_i d_I/c$, d_S and d_I being the distances from the crystal to the signal and idler mirrors, respectively.

B. Energy conservation

Let us assume, to begin with, that the pump field is monochromatic, so that

$$\sum_p N_p\omega_p U_p^*(\mathbf{x}')U_p(\mathbf{x}'')e^{i\omega_p(t'-t'')} = N_P\omega_P U_P^*(\mathbf{x}')U_P(\mathbf{x}'')e^{i\omega_P(t'-t'')}. \tag{32}$$

Then

$$\begin{aligned}\langle E_S^{(-)}(\mathbf{x},t)E_S^{(+)}(\mathbf{x},t)\rangle &= (2\pi\hbar)^2 N_P\omega_P\sum_i \omega_i\int d^3x'\chi\int d^3x''\chi U_i(\mathbf{x}')U_i^*(\mathbf{x}'')U_P^*(\mathbf{x}')U_P(\mathbf{x}'')\int_0^t dt'\int_0^t dt'' G^{(+)}\\ &\quad\times(\mathbf{x},t;\mathbf{x}',t')^* G^{(+)}(\mathbf{x},t;\mathbf{x}'',t'')e^{i(\omega_P-\omega_i)(t'-t'')}\\ &= (2\pi\hbar)^2 N_P\omega_P\sum_i \omega_i\left|\int d^3x'\chi U_i^*(\mathbf{x}')U_P(\mathbf{x}')\int_0^t dt' G^{(+)}(\mathbf{x},t;\mathbf{x}',t')e^{-i(\omega_P-\omega_i)t'}\right|^2,\end{aligned} \tag{33}$$

where, from Eq. (20),

$$\begin{aligned}&\int d^3x'\chi U_i^*(\mathbf{x}')U_P(\mathbf{x}')\int_0^t dt' G^{(+)}(\mathbf{x},t;\mathbf{x}',t')e^{-i(\omega_P-\omega_i)t'}\\ &\quad= 2\pi i\sum_s \omega_s U_s(\mathbf{x})e^{-i\omega_s t}\int d^3x'\chi U_i^*(\mathbf{x}')U_s^*(\mathbf{x}')U_P(\mathbf{x}')\int_0^t dt' e^{-i(\omega_P-\omega_i-\omega_s)t'}\\ &\quad= 2\pi i\sum_s \omega_s U_s(\mathbf{x})e^{-i\omega_s t}e^{-(i)(\omega_P-\omega_i-\omega_s)t}\frac{\sin\frac{1}{2}(\omega_P-\omega_i-\omega_s)t}{\frac{1}{2}(\omega_P-\omega_i-\omega_s)}\int d^3x'\chi U_i^*(\mathbf{x}')U_s^*(\mathbf{x}')U_P(\mathbf{x}').\end{aligned} \tag{34}$$

The integration time t multiplied by any field frequency of interest is assumed to be very large, and so the dominant contribution to (34) comes from frequencies $\omega_s = \omega_P - \omega_i$. We therefore make the familiar replacement of the sinc function by $\pi\delta(\omega_P-\omega_i-\omega_s)$:

$$\left|\int d^3x'\chi U_i^*(\mathbf{x}')U_P(\mathbf{x}')\int_0^t dt' G^{(+)}(\mathbf{x},t;\mathbf{x}',t')e^{-i(\omega_P-\omega_i)t'}\right|^2 \to (2\pi^2)^2\omega_{si}^2|U_{si}(\mathbf{x})|^2\left|\int d^3x'\chi U_i^*(\mathbf{x}')U_{si}^*(\mathbf{x}')U_P(\mathbf{x}')\right|^2, \tag{35}$$

where the subscript ''si'' is used to indicate that the ω_s-dependent quantities are to be evaluated at

$$\omega_s = \omega_P - \omega_i \equiv \omega_{si}. \tag{36}$$

Of course, this is just the condition of energy conservation in the downconversion $\omega_P \rightarrow \omega_s + \omega_i$. With this condition Eq. (33) becomes

$$\langle E_S^{(-)}(\mathbf{x},t) E_S^{(+)}(\mathbf{x},t)\rangle = (4\pi^3\hbar)^2 N_P \omega_P \sum_i \omega_i \omega_{si}^2 |U_{si}(\mathbf{x})|^2 \times \left| \int d^3x' \chi U_i^*(\mathbf{x}') U_{si}^*(\mathbf{x}') U_P(\mathbf{x}') \right|^2. \tag{37}$$

C. Momentum conservation (phase matching)

The mode functions (29)–(31) give

$$\begin{aligned} &\int d^3x' \chi U_i^*(\mathbf{x}') U_{si}^*(\mathbf{x}') U_P(\mathbf{x}') \\ &= C_i^* C_{si}^* C_P \chi \int_V d^3x' [e^{i(\mathbf{K}_P - \mathbf{k}_{si} - \mathbf{k}_i)\cdot \mathbf{x}'} \\ &\quad - e^{i(\phi_P - \phi_{si} - \phi_i)} e^{-i(\mathbf{K}_P - \mathbf{k}_{si} - \mathbf{k}_i)\cdot \mathbf{x}'} \\ &\quad + e^{i(\phi_P - \phi_{si})} e^{-i(\mathbf{K}_P - \mathbf{k}_{si} + \mathbf{k}_i)\cdot \mathbf{x}'} - e^{i\phi_P} e^{-i(\mathbf{K}_P + \mathbf{k}_{si} + \mathbf{k}_i)\cdot \mathbf{x}'} \\ &\quad + \cdots]. \end{aligned} \tag{38}$$

Here $\int_V$ denotes integration over the volume V of the crystal, or more precisely the nonlinear interaction region bathed by the pump field, and $\mathbf{K}_P$ is the wave vector for the monochromatic pump field under consideration.

We can write the integral of the first term in brackets, for instance, as

$$\int_V d^3x' e^{i(\mathbf{K}_P - \mathbf{k}_{si} - \mathbf{k}_i)\cdot \mathbf{x}'} = 8i \frac{\sin \Delta k_x L_x}{\Delta k_x} \frac{\sin \Delta k_y L_y}{\Delta k_y} \frac{\sin \Delta k_z L_z}{\Delta k_z}, \tag{39}$$

where $\Delta k_m = (\mathbf{K}_P - \mathbf{k}_{si} - \mathbf{k}_i)_m$, $m = x,y,z$, and the mth Cartesian dimension of the interaction region is assumed to run from $-L_m$ to L_m. For $\Delta k_m = 0$, $m = x,y,z$, this integral is $8iL_xL_yL_z$, whereas for $\Delta k_m \neq 0$ its maximal value is $8i/|\Delta k_x \Delta k_y \Delta k_z|$. For $L_m \gg 1/|\Delta k_m|$, therefore, the contribution to (39) from values of $\Delta k_m \neq 0$ is small compared with the contribution from $\Delta k_m = 0$. This means that the dominant contribution to (38) comes from wave vectors satisfying the momentum conservation condition

$$\mathbf{K}_P = \mathbf{k}_{si} + \mathbf{k}_i. \tag{40}$$

This phase-matching condition implies

$$n_P^2 \omega_P^2 = \omega_{si}^2 n_{si}^2 + \omega_i^2 n_i^2 + 2 n_{si} n_i \omega_{si} \omega_i \cos\Theta, \tag{41}$$

where n_P, n_{si}, and n_i are the refractive indices of the crystal for frequencies ω_P, ω_{si}, and ω_i, and Θ is the angle between $\mathbf{k}_{si}$ and $\mathbf{k}_i$ (Fig. 2). In the experiments [1] the angle Θ is fixed by the positions of the mirrors and diaphragms, and the pump frequency ω_P corresponds to the 351.1-nm line of an argon ion laser. The refractive indices n_P, n_{si}, and n_i for the $LiIO_3$ crystal employed in the experiments may be determined from the tabulations of Eimerl *et al.* [7], for instance. Therefore, to the extent that ω_P and Θ are precisely determined, Eqs. (36) and (41) uniquely determine $\omega_i \equiv \omega_I$ and $\omega_{si} \equiv \omega_S = \omega_P - \omega_I$, and therefore $\mathbf{k}_{si} \equiv \mathbf{K}_S$ and $\mathbf{k}_i \equiv \mathbf{K}_i$ (see Sec. V). And if (40) is satisfied, the contributions to (38) from all other terms but the first two in brackets will be non-phase-matched and negligible. That is,

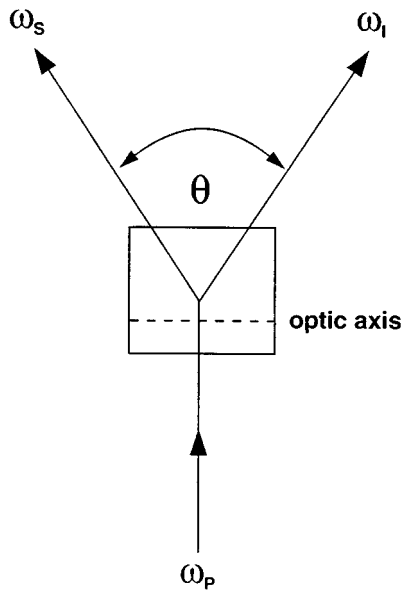

FIG. 2. The angle Θ between the created signal and idler fields is determined by angle phase matching in which the pump is linearly polarized as an extraordinary wave, incident at 90° to the optic axis of the crystal, and the signal and idler waves are linearly polarized ordinary waves.

$$\begin{aligned} &\int d^3x' \chi U_i^*(\mathbf{x}') U_{si}^*(\mathbf{x}') U_P(\mathbf{x}') \\ &\quad \rightarrow C_I^* C_S^* C_P \chi V [1 - e^{i(\phi_P - \phi_S - \phi_I)}] \end{aligned} \tag{42}$$

and therefore

$$\begin{aligned} &\langle E_S^{(-)}(\mathbf{x},t) E_S^{(+)}(\mathbf{x},t)\rangle \\ &\quad = (4\pi^3\hbar)^2 N_P \omega_P \omega_I \omega_S^2 |U_S(\mathbf{x})|^2 \\ &\quad \times |C_I C_S C_P|^2 \chi^2 V^2 |1 - e^{i(\phi_P - \phi_S - \phi_I)}|^2. \end{aligned} \tag{43}$$

D. Signal and idler counting rates

Equation (43) implies the signal counting rate

$$R_S = A_S(1 - \cos\theta), \tag{44}$$

$$\theta \equiv \phi_P - \phi_S - \phi_I = \frac{2\omega_P d_P}{c} - \frac{2\omega_S d_S}{c} - \frac{2\omega_I d_I}{c} = 4\pi \left(\frac{d_P}{\lambda_P} - \frac{d_S}{\lambda_S} - \frac{d_I}{\lambda_I} \right). \tag{45}$$

For our purposes here, A_S is an uninteresting constant. The analogous considerations for the idler counting rate give likewise

$$R_I \propto (1 - \cos\theta). \tag{46}$$

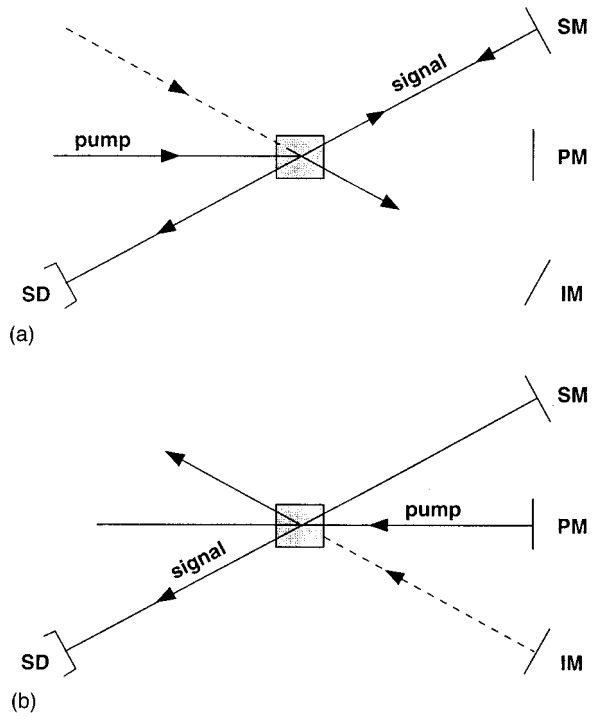

FIG. 3. Two distinct processes leading to the detection of a signal photon at SD. In (a) the signal photon to be detected is created by the forward-propagating pump, reflects off SM, and propagates back through the crystal to SD. In (b) the signal photon is created by the backward-propagating pump that has reflected off PM, and propagates directly to SD. In (a) the signal is generated by the mixing of the pump with a vacuum, forward-propagating idler field, and in (b) by the mixing of the backward-propagating pump with a vacuum, backward-propagating idler field.

These sinusoidal variations of the signal and idler count rates with the crystal-mirror separations d_P, d_S, and d_I have been observed in the experiments of Herzog *et al.* [1].

E. Physical interpretation and simplified formulation

These results can be interpreted as follows. The total probability amplitude for a photon to be counted at the detector SD (Fig. 1) is the sum of amplitudes for two distinct and indistinguishable processes. In the first of these processes the incoming pump mixes with an incoming vacuum idler to generate a signal photon which then propagates to SM and is reflected back through the crystal to SD [Fig. 3(a)]. The amplitude for this process may be taken to be $A_1 = be^{i\phi_s}$. In the second process a signal photon is created when the pump beam reflected from PM mixes with a vacuum idler field reflected from IM to generate a signal photon that then propagates from the crystal to SD [Fig. 3(b)]. Since it involves pump and idler phase changes associated with propagation between the crystal and the mirrors, but not such phase change for the signal, the amplitude for the second process is $A_2 = -be^{i(\phi_P - \phi_I)}$ [8]. Thus the probability of counting a signal photon at SD is

$$|A_1 + A_2|^2 = |b|^2 |e^{i\phi_S} - e^{i(\phi_P - \phi_I)}|^2 \propto 1 - \cos\theta, \qquad (47)$$

in agreement with (44).

The derivation just given involves interfering probability amplitudes for the two ways by which a signal photon can appear at SD, and of course the same result is obtained by considering the two interfering paths by which an idler photon can appear at ID. Because the signal and idler photons are created in pairs, as discussed further in the following section, we can obtain the same result by considering the two distinct ways in which a pump photon can be annihilated and the created signal and idler photons *both* appear at their respective detectors. One way is for the pump photon to be annihilated in the crystal without first reflecting off PM; the signal and idler photon then reflect off SM and IM and propagate to SD and ID, respectively. The amplitude for this process is, say, $-be^{i(\phi_S + \phi_I)}$ [8]. Alternatively, the pump photon can pass through the crystal, reflect off PM, and then create the signal-idler pair, and for this process we can take the amplitude to be $be^{i\phi_P}$. Adding these two amplitudes and squaring the modulus of the result then gives the signal/idler *coincidence* probability $\propto 1 - \cos\theta$.

In the derivation of (44)–(46) we have integrated over the interaction region inside the crystal, whereas the simplified derivations just given for the θ dependence of the counting rates assume in effect a point interaction. The more detailed derivation leading to (44)–(46) gives, through the integration over both time and interaction volume, the energy and momentum conservation conditions (36) and (40), respectively. These conditions are *assumed* in the simplified derivation just given. A second simplified derivation, based on field operators, can be obtained when these conditions are presumed: write

$$a_S = a_{S0} + \beta a_{P0} a_{I0}^\dagger, \quad \beta = \gamma(1 - e^{i\theta}), \qquad (48)$$

$$a_I = a_{I0} + \beta a_{P0} a_{S0}^\dagger, \qquad (49)$$

where a_S and a_I are the photon annihilation operators for the specified, phase-matched signal and idler modes S and I, respectively, and γ for our purposes is an unimportant constant associated with these modes and the crystal. The operators a_{S0}, a_{I0}, and a_{P0} are the free, unperturbed mode annihilation operators, satisfying $a_{S0}|\psi\rangle = a_{I0}|\psi\rangle = 0$ for the initial field state $|\psi\rangle$ with no signal or idler photons. Equations (48) and (49) contain the essential physical content of our more complicated equations for the full electric-field operators $E_{S,I}^{(+)}(\mathbf{x},t)$ when the energy and momentum conservation conditions are invoked *a priori* and when all largely irrelevant constants are effectively lumped together in γ.

For the initial state $|\psi\rangle$ we obtain by trivial algebra the expectation value

$$\langle a_S^\dagger a_S \rangle = |\beta|^2 \langle a_{P0}^\dagger a_{P0} a_{I0} a_{I0}^\dagger \rangle = |\beta|^2 \langle a_{P0}^\dagger a_{P0} \rangle$$
$$= N_P |\gamma|^2 |1 - e^{i\theta}|^2 \qquad (50)$$

and likewise

$$\langle a_{I0}^\dagger a_{I0} \rangle = N_P |\gamma|^2 |1 - e^{i\theta}|^2. \qquad (51)$$

The signal and idler counting rates are proportional to these quantities in this simplified formulation, which therefore also produces the experimentally observed variations with crystal-mirror separations.

IV. SIGNAL-IDLER COINCIDENCE RATE

The simplified formation based on (48) and (49) can also be used to calculate the signal-idler coincidence rate:

$$R_{SI}^{(2)} \propto \langle a_S^\dagger a_I^\dagger a_I a_S \rangle. \tag{52}$$

We assume that $|\beta|^2 N_P \ll 1$, which is consistent with the assumption of an undepleted pump beam. Then some simple algebra gives the result, under this assumption,

$$R_{SI}^{(2)} \propto |\beta|^2 \langle a_{P0}^\dagger a_{P0} a_{I0} a_{I0}^\dagger a_{I0} a_{I0}^\dagger \rangle = |\beta|^2 N_P$$
$$= N_P |\gamma|^2 |1 - e^{i\theta}|^2. \tag{53}$$

This result exhibits exactly the sinusoidal variations of the coincidence rate with crystal-mirror separations observed experimentally [1]. Since the more detailed theory leading to (44)–(46) merely reproduces this result of the simplified formulation, we will not bother to carry it through. It should be emphasized, however, that the coincidence rate is directly proportional to the single-photon counting rate, and in particular has the same dependence on the mirror-crystal separations, showing clearly that we are dealing with a photon-pair effect whereby photons are created in pairs.

Classical formulation

Some aspects of these results are understandable classically. In a classical field formulation the operators a_S and a_I are replaced by c numbers α_S and α_I. The classical analogs of expressions (48) and (49) are

$$\alpha_S = \alpha_{S0} + \beta \alpha_{P0} \alpha_{I0}^*, \tag{54}$$

$$\alpha_I = \alpha_{I0} + \beta \alpha_{P0} \alpha_{S0}^*. \tag{55}$$

The classical quantity corresponding to Eq. (50) is the squared modulus of the signal field amplitude:

$$|\alpha_S|^2 = |\alpha_{S0}|^2 + |\beta|^2 |\alpha_{P0}|^2 |\alpha_{I0}|^2 + 2\,\mathrm{Re}(\beta \alpha_{P0} \alpha_{S0}^* \alpha_{I0}^*)$$
$$= |\beta|^2 |\alpha_{P0}|^2 |\alpha_{I0}|^2 \propto |1 - e^{i\theta}|^2 \tag{56}$$

if $\alpha_{S0} = 0$, i.e., if the signal field is initially zero while both the idler and pump fields have some initial energy. In other words, if we assume that the initial signal field is zero, then we can obtain classically the same variation of the generated signal energy with θ as is obtained quantum mechanically for the signal photon count.

Similarly, from (55),

$$|\alpha_I|^2 = |\alpha_{I0}|^2 + |\beta|^2 |\alpha_{P0}|^2 |\alpha_{S0}|^2 + 2\,\mathrm{Re}(\beta \alpha_{P0} \alpha_{I0}^* \alpha_{S0}^*)$$
$$= |\beta|^2 |\alpha_{P0}|^2 |\alpha_{S0}|^2 \propto |1 - e^{i\theta}|^2 \tag{57}$$

if we take $\alpha_{I0} = 0$ but α_{P0}, $\alpha_{S0} \neq 0$. That is, we can obtain the same variation of $|\alpha_I|^2$ with θ as is obtained quantum mechanically for the idler photon count if we assume that there is initially no idler energy but that the initial signal and pump fields are both nonvanishing.

We will not elaborate further on classical themes [9], except to note that a coincidence rate analogous to (53) cannot be inferred from a consistent classical theory. The classical counterpart of $R_{SI}^{(2)}$ is

$$|\alpha_S|^2 |\alpha_I|^2 \cong |\alpha_{S0}|^2 |\alpha_{I0}|^2 + |\alpha_{P0}|^2 |\beta|^2 (|\alpha_{I0}|^4 + |\alpha_{S0}|^4)$$
$$+ 2\,\mathrm{Re}[\alpha_{P0} \alpha_{S0}^* \alpha_{I0}^* |\beta|^2 (|\alpha_{I0}|^2 + \beta |\alpha_{S0}|^2)] \tag{58}$$

in the same approximation made in (53) of retaining only terms up to quadratic in χ. It is evident from these results that a classical theory cannot *consistently* capture all aspects of the quantum-mechanical and experimentally observed results. Thus, we obtain $|\alpha_I|^2 \propto |1 - e^{i\theta}|^2$ and $|\alpha_I|^2 |\alpha_S|^2 \propto |1 - e^{i\theta}|^2$ by choosing $\alpha_{I0} = 0$, but then we do not get $|\alpha_S|^2 \propto |1 - e^{i\theta}|^2$.

V. EFFECTS OF PARTIAL TEMPORAL COHERENCE

In obtaining the results for the variations of the signal, idler, and coincidence counts with crystal-mirror separations, we have assumed that the pump is perfectly monochromatic and that the signal and idler photons are monochromatic and independent of the filters and diaphragms employed in the actual experiments. We will now consider what happens when the pump has finite temporal coherence and when there is some frequency spread in the measured signal and idler photons [10]. Both these effects will reduce the interference between the two processes indicated in Fig. 3. Since they are physically distinct effects, we will consider them separately.

A. Pump coherence

Beginning with Eq. (32), our analysis in Sec. IV assumed that the pump field incident on the crystal has a precisely defined frequency ω_P and wave vector $\mathbf{K}_P$. Suppose instead that there is a distribution of pump frequencies about ω_P. We write $\omega_p = \omega_P + \Delta_p$ and replace (32) by

$$\sum_p N_p \omega_p U_p^*(\mathbf{x}') U_p(\mathbf{x}'') e^{i\omega_p (t' - t'')} = N_P \omega_P e^{i\omega_P (t' - t'')} \int_{-\infty}^{\infty} d\Delta_p g(\Delta_p) U_p^*(\mathbf{x}') U_p(\mathbf{x}'') e^{i\Delta_p (t' - t'')}, \tag{59}$$

where $g(\Delta_p)$ is some narrow, normalized distribution function, peaking at $\Delta_p = 0$, whose width is a measure of the degree of nonmonochromaticity and temporal incoherence of the incident pump field.

It is straightforward to carry through the analysis of Sec. IV starting from (59) instead of (32). We obtain instead of (37), for instance, the expression

$$\langle E_S^{(-)}(\mathbf{x},t) E_S^{(+)}(\mathbf{x},t) \rangle = (4\pi^3 \hbar)^2 N_P \omega_P \int_{-\infty}^{\infty} d\Delta_p g(\Delta_p) \sum_i \omega_i \omega_{si}^2 |U_{si}(\mathbf{x})|^2 \left| \int d^3x' \chi U_i^*(\mathbf{x}') U_{si}^*(\mathbf{x}') U_p(\mathbf{x}') \right|^2, \tag{60}$$

where energy conservation now takes the form

$$\omega_i+\omega_{si}=\omega_P+\Delta_p. \tag{61}$$

The integral over the crystal interaction volume leads similarly to the momentum conservation condition $\mathbf{k}_i+\mathbf{k}_{si}=\mathbf{K}_p$, where $\mathbf{K}_p$ now has magnitude $n(\omega_p)\omega_p/c\cong n(\omega_P)(\omega_P+\Delta_p)/c$. (We assume that all wave vectors associated with the incident pump point in the same direction.) With these energy and momentum conservation conditions, Eq. (60) takes the form

$$\langle E_S^{(-)}(\mathbf{x},t)E_S^{(+)}(\mathbf{x},t)\rangle\propto\int_{-\infty}^{\infty}d\Delta_p g(\Delta_p)[1-\cos\theta(\Delta_p)], \tag{62}$$

$$\theta(\Delta_p)\equiv 2(\omega_P+\Delta_p)d_P/c-2\omega_i d_I/c-2\omega_{si}d_S/c. \tag{63}$$

It is convenient to write $\omega_i=\omega_I+\Delta_i$ and $\omega_{si}=\omega_S+\Delta_s$, with $\omega_S+\omega_I=\omega_P$, so that

$$\Delta_i+\Delta_s=\Delta_p. \tag{64}$$

Assuming $|\Delta_i|/\omega_I,|\Delta_s|/\omega_S\ll 1$, and $n_{si}\cong n_S$, $n_i\cong n_I$, the momentum conservation condition on the frequencies Δ_i and Δ_s can be obtained from (41) by differentiation:

$$n_P^2\omega_P\Delta_p=n_S^2\omega_S\Delta_s+n_I^2\omega_I\Delta_i+n_S n_I(\omega_S\Delta_i+\omega_I\Delta_s)\cos\Theta. \tag{65}$$

Equations (64) and (65) determine the deviations Δ_s and Δ_i of the created signal and idler photons from ω_S and ω_I, given the deviation Δ_p of the pump frequency from $\omega_P=\omega_S+\omega_I$.

Before calculating Δ_s and Δ_i in terms of Δ_p, let us return to the equations

$$\omega_S+\omega_I=\omega_P, \tag{66}$$

$$n_P^2\omega_P^2=n_S^2\omega_S^2+n_I^2\omega_I^2+2n_S n_I\omega_S\omega_I\cos\Theta \tag{67}$$

determining ω_S and ω_I. In the experiments of Herzog *et al.* [1] the angle Θ is such that a 351.1-nm pump generates 632.8- and 788.7-nm signal and idler fields, respectively. A type-I phase matching is employed, such that the pump is a linearly polarized extraordinary wave incident at 90° to the optic axis, while the signal and idler are both linearly polarized ordinary waves (Fig. 2). For these wavelengths and polarizations we calculate, from the data of Eimerl *et al.* [7], $n_P=1.7197$, $n_S=1.8810$, and $n_I=1.8657$ for $LiIO_3$. Then we can infer the angle Θ from Eq. (67):

$$\Theta=\cos^{-1}(0.6797)=47.2°. \tag{68}$$

Knowing Θ, we can now solve Eqs. (64) and (65) relating Δ_s and Δ_i to Δ_p, the result being

$$\Delta_s=0.56\Delta_p\equiv\xi_s\Delta_p, \tag{69}$$

$$\Delta_i=0.44\Delta_p\equiv\xi_i\Delta_p. \tag{70}$$

Thus

$$\begin{aligned}\theta(\Delta_p)&=2(\omega_P+\Delta_p)d_P/c-2(\omega_S+\Delta_s)d_S/c\\&\quad-2(\omega_I+\Delta_i)d_I/c\\&=\theta+2\Delta_p(d_P-\xi_i d_I-\xi_s d_S)/c,\end{aligned} \tag{71}$$

where $\theta=2\omega_P d_P/c-2\omega_S d_S/c-2\omega_I d_I/c$ is the value of the net phase difference when the pump is perfectly monochromatic. Expression (62) is then

$$\begin{aligned}\langle E_S^{(-)}(\mathbf{x},t)E_S^{(+)}(\mathbf{x},t)\rangle&\propto\int_{-\infty}^{\infty}d\Delta_p g(\Delta_p)-\mathrm{Re}\left(e^{i\theta}\int_{-\infty}^{\infty}d\Delta_p g(\Delta_p)e^{2i\Delta_p(d_P-\xi_s d_S-\xi_i d_I)/c}\right)\\&=1-\mathrm{Re}\left(e^{i\theta}\int_{-\infty}^{\infty}d\Delta_p g(\Delta_p)e^{2i\Delta_p(d_P-\xi_s d_S-\xi_i d_I)/c}\right).\end{aligned} \tag{72}$$

In order to have a simple integral we take the frequency distribution of the pump to be Lorentzian:

$$g(\Delta_p)=\frac{\beta_p/\pi}{\Delta_p^2+\beta_p^2}, \tag{73}$$

where β_p is the bandwidth (HWHM). This gives

$$\begin{aligned}&\int_{-\infty}^{\infty}d\Delta_p g(\Delta_p)e^{2i\Delta_p(d_P-\xi_s d_S-\xi_i d_I)/c}\\&\quad=e^{-2\beta_p|d_p-\xi_s d_S-\xi_i d_I|/c}=e^{-|d_P-\xi_s d_S-\xi_i d_I|/L_p},\end{aligned} \tag{74}$$

and therefore

$$\langle E_S^{(-)}(\mathbf{x},t)E_S^{(+)}(\mathbf{x},t)\rangle=1-e^{-|d_P-\xi_s d_S-\xi_i d_I|/L_p}\cos\theta, \tag{75}$$

where we define $L_p=c/2\beta_p$ to be the coherence length of the pump field. Note that if $d_S\cong d_I\equiv d$, then

$$|d_P-\xi_s d_S-\xi_i d_I|/L_c\cong|d_P-(\xi_s+\xi_i)d|/L_c\cong|d_P-d|/L_c. \tag{76}$$

These results for the effect of the pump coherence length are consistent with the observation of Herzog *et al.* that ''the crystal-mirror path length for the pump should not differ by more than the coherence length of the pump (a few meters in [the] experiment) from the distances from the crystal to the signal and idler mirror'' [1].

B. Signal-idler coherence length

In the experiments [1] two diaphragms of diameter ≈ 0.8 mm, separated by 90 cm, are placed in the paths of both the signal and idler fields between the crystal and the detectors. This ensures that the detected signal and idler modes propagate nearly unidirectionally. Nevertheless there remains some effective spread $\Delta\Theta \approx (0.4/900) = 4.45 \times 10^{-4}$ rad in the angle Θ. This spread allows a distribution of phase-matched signal and idler frequency pairs ω_s and ω_i (Fig. 4).

If we assume again a monochromatic pump (i.e., $\Delta_p = 0$), so that $\Delta_i = -\Delta_s$ [Eq. (64)], then (41) implies

$$\begin{aligned} 0 &\cong n_S^2 \omega_S \Delta_S + n_I^2 \omega_I \Delta_I + n_S n_I (\omega_S \Delta_i + \omega_I \Delta_s)\cos\Theta \\ &\quad - n_S n_I \omega_S \omega_I \sin\Theta \, \Delta\Theta \\ &= [n_S^2 \omega_S - n_I^2 \omega_I + n_S n_I (\omega_I - \omega_S)\cos\Theta]\Delta_s \\ &\quad - n_S n_I \omega_S \omega_I \sin\Theta \, \Delta\Theta . \end{aligned} \tag{77}$$

In other words, the deviation Δ_s from ω_S of signal photons, arising from a deviation $\Delta\Theta$ from the angle Θ for which there is phase matching for ω_S and ω_I photons, is

$$\Delta_s = \frac{n_S n_I \omega_S \omega_I \sin\Theta \, \Delta\Theta}{n_S^2 \omega_S - n_I^2 \omega_I + n_S n_I (\omega_I - \omega_S)\cos\Theta} \equiv \eta \Delta\Theta, \tag{78}$$

and consequently $\Delta_i = -\eta\Delta\Theta$. Based on the numbers already used for the angle Θ and the refractive indices, we obtain $\eta \cong 2.3 \times 10^{16}\ \mathrm{s}^{-1}$ and therefore

$$\Delta_s \cong (2.3 \times 10^{16}\ \mathrm{s}^{-1})(4.45 \times 10^{-4}) = 1.0 \times 10^{13}\ \mathrm{s}^{-1}, \tag{79}$$

giving the order-of-magnitude estimate $2\pi c/\Delta_s \approx 189\ \mu$m for the signal-idler coherence length, in qualitative agreement with the experimental result $\approx 260\ \mu$m [1].

To see how this signal-idler coherence length affects the measured counts as a function of mirror-crystal separations, we return to Eq. (37). The integration over volume, together with the fact that there is now a distribution of phase-matched $\mathbf{k}$ vectors and therefore a distribution of created signal and idler frequency pairs according to (78), leads from (37) to

$$\langle E_S^{(-)}(\mathbf{x},t) E_S^{(-)}(\mathbf{x},t) \rangle \propto \int_{-\infty}^{\infty} d\Delta_s f(\Delta_s) |1 - e^{i\theta(\Delta_s)}|^2, \tag{80}$$

$$\begin{aligned} \theta(\Delta_s) &\equiv \phi_P - 2(\omega_S + \Delta_s) d_S/c - 2(\omega_I - \Delta_s) d_I/c \\ &= \phi_P - \phi_S - \phi_I - 2\Delta_s (d_S - d_I)/c \\ &= \theta - 2\Delta_s (d_S - d_I)/c, \end{aligned} \tag{81}$$

instead of the result (43) obtained under the assumption $\Delta\Theta = 0$. We have introduced in (80) a normalized distribution function $f(\Delta_s)$ for the frequency deviations Δ_s consistent with phase matching. Once again we assume a Lorentzian and obtain

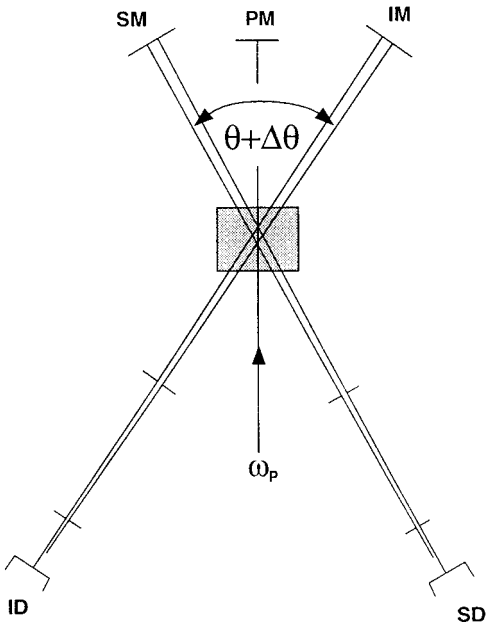

FIG. 4. Apertures are placed in both the signal and idler paths in the experiments of Herzog *et al.* [1]. The diameter of each aperture is 0.8 mm, and each aperture pair is separated by 90 cm. This gives an angular spread $\Delta\Theta \sim 0.4/900 = 4.45 \times 10^{-4}$ rad that in turn gives rise to finite bandwidths of phase-matched signal-idler pairs.

$$\begin{aligned} &\langle E_S^{(-)}(\mathbf{x},t) E_S^{(+)}(\mathbf{x},t) \rangle \\ &\quad \propto 1 - \mathrm{Re}\left(e^{i\theta} \int_{-\infty}^{\infty} d\Delta_s f(\Delta_s) e^{-2i\Delta_s (d_S - d_I)/c} \right) \\ &\quad = 1 - e^{-2\beta_s |d_S - d_I|/c} \cos\theta, \end{aligned} \tag{82}$$

which replaces (44) when the bandwidth $\beta_s = 0$. Here β_s is the width of the Lorentzian function $f(\Delta_s)$, analogous to the width β_p of (73). Our result is consistent with the experimental observation of Herzog *et al.*: ''it is . . . the *relative* position of signal and idler mirror which has to lie within the coherence length of the spontaneously emitted down-converted light ($\approx 260\ \mu$m in our experiment)'' [1].

VI. SUMMARY

Starting from the Hamiltonian (4) for general three-wave mixing, and treating all fields quantum mechanically, we have derived the experimentally observed results of Herzog *et al.* [1] for the variation with crystal-mirror separations of signal and idler counts and coincidence counts. Allowing for nonmonochromaticity of the incident pump, and a distribution of phase-matched signal and idler frequency pairs associated with a spread in phase-matching angles, we have also accounted for the observed dependences of the counting rates on the pump and signal-idler coherence lengths.

The theory presented here, which allows for a finite interaction volume, validates the interpretation of Herzog *et al.* [1] that the experiment indicated in Fig. 1 represents a generalization of cavity QED experiments to a situation where

the separation between the emitter and mirrors greatly exceeds the wavelength. In a sense the emitter in this case still acts as a point source, as in ordinary cavity QED; this is a consequence of the phase-matching (momentum conservation) conditions ensuing from an integration over all ''point sources'' in the volume where the three-wave mixing takes place.

ACKNOWLEDGMENTS

A.Z. would like to acknowledge financial support by the Austrian Science Foundation FWF, Grant No. S6502, and by the National Science Foundation under Grant No. PHY 92-13964. H.F.'s work at Los Alamos was supported in part by Associated Western Universities.

[1] T. J. Herzog, J. G. Rarity, H. Weinfurter, and A. Zeilinger, Phys. Rev. Lett. **72**, 629 (1994).

[2] See, for instance, S. Haroche and D. Kleppner, Phys. Today **42** (1), 24 (1989); E. A. Hinds, in *Advances in Atomic, Molecular, and Optical Physics*, edited by D. R. Bates and B. Bederson (Academic, Boston, 1990), Vol. 28; *Cavity Quantum Electrodynamics*, edited by P. R. Berman (Academic, San Diego, 1994).

[3] See, for instance, P. W. Milonni, *The Quantum Vacuum, An Introduction to Quantum Electrodynamics* (Academic, San Diego, 1994).

[4] See, for instance, J. D. Jackson, *Classical Electrodynamics* (Wiley, New York, 1975), pp. 158–161.

[5] C. K. Hong and L. Mandel, Phys. Rev. A **31**, 2409 (1985).

[6] See, for instance, F. Zernike and J. E. Midwinter, *Applied Nonlinear Optics* (Wiley, New York, 1973).

[7] D. Eimerl, S. Velsco, L. Davis, and F. Wang, Prog. Cryst. Growth Charact. **20**, 59 (1990).

[8] The minus sign here is rather arbitrary, and is introduced in order to obtain the minus sign before the $\cos\theta$ factor in (47). This is essentially the same minus sign that appears between counterpropagating waves in the mode functions (29)–(31). The comparison with experiment is not sensitive to this sign, as only the sinusoidal variations with mirror separations are measured.

[9] See, I. R. Senitzky, Phys. Rev. Lett. **73**, 3040 (1994); T. Herzog, J. Rarity, H. Weinfurter, and A. Zeilinger, *ibid.* **73**, 3041 (1994).

[10] Effects of pump coherence have been treated in various contexts in nonlinear optics by other authors. See, for instance, the discussion in D. N. Klyshko, *Photons and Nonlinear Optics* (Gordon and Breach, New York, 1989).